Available online at www.sciencedirect.com
ScienceDirect
International Journal of Heat and Mass Transfer 51 (2008) 1179–1191
International Journal of HEAT and MASS TRANSFER
www.elsevier.com/locate/ijhmt

Numerical study on laminar convection heat transfer in a rectangular channel with longitudinal vortex generator. Part A: Verification of field synergy principle

J.M. Wu [a,b], W.Q. Tao [a,*]

[a] State Key Laboratory of Multiphase Flow in Power Engineering, School of Energy and Power Engineering, Xi'an Jiaotong University, Xi'an City 710049, China
[b] School of Environment and Chemical Engineering, Xi'an Polytechnic University, Xi'an City 710048, China

Received 12 October 2005; received in revised form 17 March 2007
Available online 25 May 2007

Abstract

This study presents numerical computation results on laminar convection heat transfer in a rectangular channel with a pair of rectangular winglets longitudinal vortex generator punched out from the lower wall of the channel. The effect of the punched holes and the thickness of the rectangular winglet pair to the fluid flow and heat transfer are numerically studied. It is found that the case with punched holes has more heat transfer enhancement in the region near to the vortex generator and lower average flow frictional coefficient compared with the case without punched holes. The thickness of rectangular winglet can cause less heat transfer enhancement in the region near to the vortex generator and almost has no significant effect on the total pressure drop of the channel. The effects of Reynolds number (from 800 to 3000), the attack angle of vortex generator (15°, 30°, 45°, 60° and 90°) were examined. The numerical results were analyzed from the viewpoint of field synergy principle. It was found that the essence of heat transfer enhancement by longitudinal vortex can be explained very well by the field synergy principle, i.e., when the second flow generated by vortex generators results in the reduction of the intersection angle between the velocity and fluid temperature gradient, the heat transfer in the present channels will be enhanced. Longitudinal vortices (LVs) improve the synergy between velocity and temperature field not only in the region near LVG but also in the large downstream region of longitudinal vortex generator. So LVs enable to enhance the global heat transfer of channel. Transverse vortices (TVs) only improve the synergy in the region near VG. So TVs can only enhance the local heat transfer of channel.

Keywords: Rectangular winglet; Longitudinal vortex; Heat transfer enhancement; Field synergy principle

1. Introduction

The compact heat exchanger is widely used in such fields as automobile industry, heating and air conditioning, power system, chemical engineering, electronic chip cooling and aerospace, etc. The subject of heat transfer enhancement is of significant interest in developing compact heat exchanger to meet the desire of high efficiency and low cost with the volume as small as possible and the weight as light as possible. A large amount of investigations have been carried out in this area since 1960s [1].

It is well known that the thermal resistance of gas is inherently higher than that of liquid and two-phase flow. Specially designed fin surfaces are often the most interesting method to enhance the gas side heat transfer of the compact heat exchanger. The role of the fin is of twofold. First it increases the area of heat transfer surface. Second it is also expected to establish a higher heat transfer coefficient of the gas side by increasing disturbances or decreasing the thermal boundary layer. Based on this idea, the fin surface may be periodically interrupted such as the wavy fin, louver fin or slotted fin surfaces in the main flow

* Corresponding author. Tel./fax: +86 29 82669106.
E-mail address: wqtao@mail.xjtu.edu.cn (W.Q. Tao).

0017-9310/$ - see front matter © 2007 Published by Elsevier Ltd.
doi:10.1016/j.ijheatmasstransfer.2007.03.032

Nomenclature

a	transverse space between the winglet pair defined in Fig. 3 (m)
B	width of channel (m)
b	thickness of vortex generator (m)
c_p	specific heat of fluid (J/(kg K))
D_e	hydraulic diameter of rectangular duct (m)
DWVG	delta winglet vortex generator
f	fanning frictional factor
G_y	node number in y-direction
G_z	node number in z-direction
h	height of vortex generator (m)
H	height of channel (m)
l	length of longitudinal vortex generator, wetting perimeter (m)
L	length of channel (m)
LV	longitudinal vortex
LVG	longitudinal vortex generator
Nu	Nusselt number
p	static pressure (Pa)
Pr	Prandtl number
Re	Reynolds number
RWLVG	rectangular winglet longitudinal vortex generator
s	streamwise coordinate of LVG defined in Fig. 2 (m)
T	temperature (K)
TV	transverse vortex
u	velocity in x-direction (m/s)
U	dimensionless velocity vector
v	velocity in y-direction (m/s)
VG	vortex generator
w	velocity in z-direction (m/s)
x, y, z	Cartesian co-ordinates
x_{in}	entrance length of velocity boundary layer (m)

Greek symbols

β	attack angle of LVG (deg.)
Δp	pressure drop in Δx (Pa)
ΔT	temperature difference (K)
Δx	tiny distance in streamwise direction (m)
λ	thermal conductivity (W/m K)
η	kinetic viscosity (kg/m s)
θ	synergy angle (deg.)
Θ	dimensionless temperature
ρ	density (kg/m^3)
Φ	heat transfer rate (W/m^2 K)

Subscripts

b	bulk
in	inlet
i, k	index
m	average
x	local
w	wall
0	channel without vortex generator

direction to disturb the flow and enhance the heat transfer. The vortex generator (VG) can be regarded as a special kind of extended surface, which can be stamped on or punched out from the fin. Although the heat transfer surface area may not be changed before and after the set up of VG, the fluid flow can be strongly disturbed because of the generation of vortex when fluid flows over it. In the conventional point of view, vortex generator not only disturbs the flow field, disrupt the growth of the boundary layer, but also makes fluid swirling and causes a heavy exchange of core and wall fluid, leading to the enhancement of heat transfer. The vortex may be divided into transverse vortex (TV) and longitudinal vortex (LV) according to its rotating axis direction. The axes of TVs lie perpendicular to the main flow direction, while LVs have their axes parallel to the main flow direction, thus they are also called streamwise vortices. In general, the LVs have been reported to be more efficient than TVs for heat transfer enhancement [2].

2. Brief review of previous work

The early report on longitudinal vortex in boundary layer control was presented by Schubauer and Spangenberg [3] in which the LVs were used to delay boundary layer separation on aircraft wings. The research on heat transfer related to VG was firstly reported by Johnson and Joubert [4]. The authors conducted the heat transfer of a circular cylinder in cross-flow with delta winglet vortex generators (DWVG) located at a fixed angular position on the cylinder. The test results showed that the local Nusselt number at that position was increased as much as 200%, while the overall Nusselt number was not increased because of the decreases elsewhere on the cylinder. It was explained that the enhanced thermal mixing resulted in the local enhancement. The followed researches on the heat transfer enhancement of the LV mainly focused on the external flow. The researches included a VG, a pair of VGs or two rows of VGs embedded in a laminar or turbulent boundary layer [5–7], and the effects of the LVs on the local and downstream heat transfer were analyzed. Shizawa and Eaton [8] carried out an experiment of a single vortex in a pressure-driven 3-D turbulent boundary layer. The experimental results indicated that the rotating direction of vortex was very important in its interaction with the boundary layer. If the vortex induced a flow near the wall in the same direction as the transverse velocity of the boundary layer, the

perturbations induced by the vortex in the boundary layer would decay quickly. Otherwise, if the vortex induced a velocity near the wall in the opposed direction with the transverse flow in the boundary layer, then this boundary layer perturbations might persist. Therefore, it can be seen that the LV fully changes the flow structure, and it should be considered carefully if a turbulence flow with LV is predicted or simulated by the traditional turbulence model [9].

Fiebig et al. [10] presented a study on the VGs in the form of one delta wing and one pair of delta winglets in a rectangular channel with Reynolds number from 1360 to 2270 by employing the unsteady liquid crystal thermography method. They concluded that the local heat transfer was enhanced up to 200% and the delta wing caused the highest local enhancement. When Reynolds number was 1360, the Colburn j factor was increased by 20–60%. Based on this interesting work, Fiebig et al. [11] systematically studied the performance of four different kinds of LVGs(delta wing, delta winglet pair, rectangular wing and rectangular winglet pair) in the developing laminar rectangular channel flow. The Reynolds numbers in this study were between 1000 and 2000. Stable LVs were found up to much higher angles of attack than corresponding wings in free stream. The drag induced by VG was found to be nearly proportional to the angle of attack and independent of the Reynolds number or VG shape. Local heat transfer augmentation of several 100% and mean heat transfer enhancement of more than 50% over an area more than 50 times the VG area were achieved. For per unit LVG area, the delta wing provided the best effectiveness of the heat transfer enhancement, the next was delta winglet, and then rectangular winglet, and the last one was rectangular wing. For the same geometry shape and constant wing area of LVGs, the heat transfer enhancement was a function of aspect ratio. The optimum heat transfer enhancement was found for aspect ratios between 1.5 and 2.0. In the practical heat exchanger, the ratio of length to height for a finned channel is at least 30 and there are multi-rows of LVGs, not necessary only one LVG. Tiggelbeck et al. [12] further experimentally studied the flow structure, heat transfer and drag force of LVs generated by two aligned rows of delta winglet pairs in a rectangular channel flow. Vortices generated by the second row showed less stable than those generated by the first row. Also, the heat transfer enhancement was larger in the downstream of the second row than that of the first row. This fact shows that the vortices generated by the first row LVGs enhanced the strength of those generated by the second row LVGs. They also observed that the peak value of the spanwise averaged Nusselt number at the downstream of the second row was strongly dependent on the spacing of the two rows.

With the rapid development of the numerical simulation technology, the investigation on the heat transfer enhancement of LVs is no longer only performed by experiment, it is also conducted by numerical simulation so that the study process may be accelerated and the cost may be decreased. The references of numerical simulation on the heat transfer enhancement of LVs in a laminar channel flow include those of Biswas et al. [13–15], Fiebig et al. [16], Saha et al. [17], Sohankar and Davidson [18], and Chung et al. [19], etc. Biswas et al. [13] presented the numerical simulation on developing laminar mixed convection in a rectangular channel with wing-type VGs at Reynolds numbers of 500 and 1815, Grashof numbers of 0.0, 2.5×10^5 and 5×10^5, and angles of attack of 20° and 26°. In their simulation, the channel wall did not have a hole under the wing. In their following simulation [14], the effect of the hole was considered, however the thickness of wing was neglected. Biswas et al. [15] presented a study on the flow structure behind a winglet type vortex generator placed in a fully developed laminar channel flow. Again the hole and the thickness of the winglet were not considered. Fiebig et al. [16] Numerically studied a developing forced convection laminar channel flow with punched delta wing and delta winglet pairs. The numerical results showed that the vortices induced the transverse velocity on the order of the streamwise velocity. Interaction of the vortices with the wall distorted the vortex cross-section from a circular to elliptical shape and caused vortex pairs spreading. Saha et al. [17] studied the vortex structures and kinetic energy budget in two-dimensional flow past a square cylinder at a Reynolds number of 100. The flow in the wake was found to be unsteady with a strong periodic component. Sohankar and Davidson [18] investigated a channel flow and heat transfer with inclined block shape vortex generators mounted on the channel wall. There were no hole on the wall, and the effect of block thickness was considered. Chung et al. [19] investigated the combined effect of angle of attack and louver angle of a winglet pair on heat transfer enhancement. The punched holes were considered but the thickness of the winglet pair was neglected. Results showed that the best performance is achieved when the angle of attack was 30° and the louver angle was 15°.

Through the above brief review on the state-of-the-art of the heat transfer enhancement by longitudinal vortices, it can be concluded that the heat transfer can be enhanced by the vortices generated by VGs. The mechanism of heat transfer enhancement is explored from the traditional points of view, which can be summarized by either decreasing the thickness of the developing boundary layer, or increasing the swirl and flow destabilization. In the present study, the laminar convection heat transfer in a rectangular channel with LVG is numerically computed to explore the essence of the heat transfer enhancement based on the field synergy principle. Our studies will be presented by two parts: the present paper is part A which provides that the heat transfer enhancement is due to the improvement of the field synergy between the velocity and temperature gradient; the effects of the geometric sizes and shapes of the LVGs on the heat transfer, field synergy and flow loss will be presented in part B [20].

3. Numerical method of the laminar convection heat transfer in a rectangular channel and its verification

As mentioned before, LVG can be stamped or mounted on the fin surface as a special heat transfer structure. However, from the view of practical application, it is convenient to punch the LVG out from the fin sheet directly. So there exist holes on the channel walls. Although the thickness of LVG is much smaller compared with the fin channel height, it should have some effects on the heat transfer and flow resistance of channel. However, to the authors' knowledge, the thickness of LVG was often neglected, and the holes under the LVG were seldom considered in the simulations of channel flow and heat transfer with LVG in the published literatures. Almost no literature considered the thickness of LVG and the holes at the same time. In the present paper, the effects of the thickness of LVG and the punched holes under the LVG will be simultaneously considered. As a preliminary study, the laminar flow and heat transfer in a rectangular duct is numerically simulated to verify the following numerical strategy.

3.1. Mathematical models for the laminar flow and heat transfer in channel

The governing equations for the laminar convection heat transfer include continuity, momentum and energy equations as followings.

Continuity equation:

$$\frac{\partial}{\partial x_i}(\rho u_i) = 0 \tag{1}$$

Momentum equation:

$$\frac{\partial}{\partial x_i}(\rho u_i u_k) = \frac{\partial}{\partial x_i}\left(\eta \frac{\partial u_k}{\partial x_i}\right) - \frac{\partial p}{\partial x_k} \tag{2}$$

Energy equation:

$$\frac{\partial}{\partial x_i}(\rho u_i T) = \frac{\partial}{\partial x_i}\left(\frac{\lambda}{c_p}\frac{\partial T}{\partial x_i}\right) \tag{3}$$

Apart from the governing equations, the related boundary conditions should be provided. There exists some differences about the inlet and outlet boundary conditions in the open references in which the flow and heat transfer in a rectangular channel with LVG were simulated. Biswas et al. [15] and Chung et al. [19] imposed uniform temperature and fully developed velocity profile for axial velocity at the channel inlet to simulate a fully developed flow. Biswas et al. [15] set the second order derivative of all velocity components and temperature to be zero at the channel outlet and Chung et al. [19] employed Neumann boundary condition at the channel outlet. Sohankar and Davidson [18] used uniform temperature and axial velocity at the channel inlet, convective boundary condition for axial velocity and Neumann condition for other velocity components and temperature at outlet to simulate a developing flow. In the present paper, the computational domain will be extended upstream and downstream so that the uniform inlet boundary condition and fully developed outlet boundary condition can be used reasonably. This is a very successful practice first suggested in [21].

3.2. Numerical simulation of the flow and heat transfer in a rectangular duct

The duct has a ratio of width of B to height of H of the cross-section, $B/H = 4.0$, a ratio of length of L to hydraulic diameter of $D_e\left(=\frac{2\times B\times H}{(B+H)}\right)$, $L/D_e = 25$. Constant temperature is assigned to the duct walls. Reynolds number based on the inlet axial velocity and hydraulic diameter of the duct is 400. The fluid is air. According to [22], the entrance length of the velocity boundary layer in the duct is about $x_{in}/D_e = 20$. So the flow and heat transfer in the duct will evolve from the inlet uniform flow to the outlet developed flow.

Due to the geometric symmetry only a quarter of the duct as shown in Fig. 1a is chosen as the computational

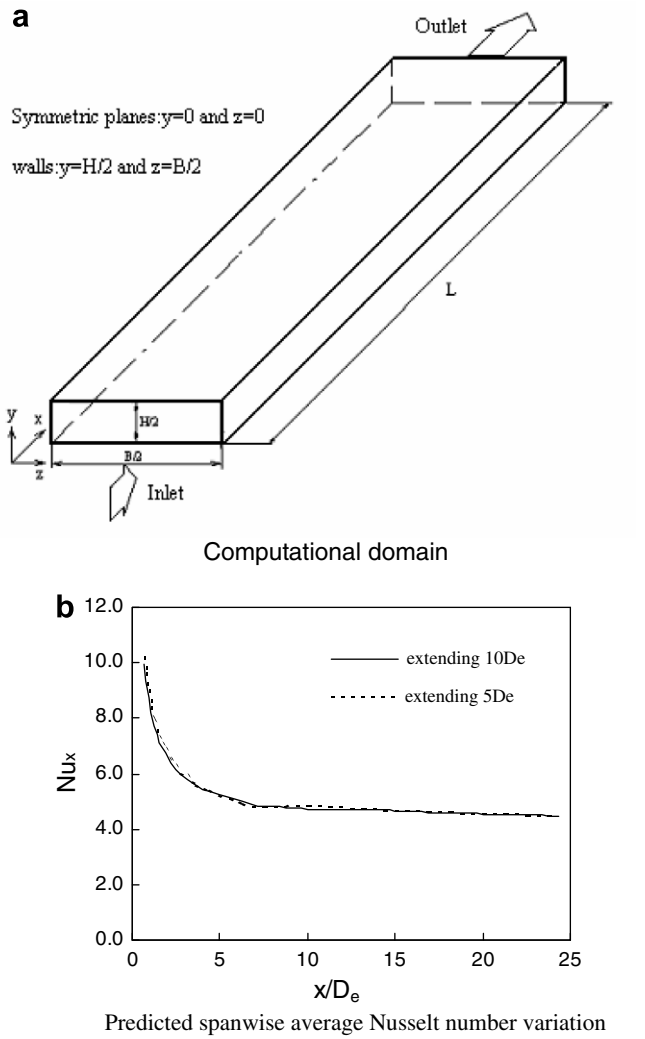

Fig. 1. Computational domain of the rectangular duct and the predicted spanwise average Nusselt number variation.

domain. In Fig. 1a, x, y, and z are streamwise, normal, and spanwise coordinates, respectively. The numerical results are compared with the theoretical solution given in [22].

A commercial computational fluid dynamics code (FLUENT) is used to simulate the flow field. Non-uniform structured meshes are generated by Gambit in which the grids near the walls are fine enough. Second order upwind scheme is used to discretize the convective term of the governing equations, and central difference scheme is employed for the diffusion term. SIMPLEC algorithm [23] is adopted to implement the coupling between pressure and velocity. As demonstrated in [24,25], the SIMPLEC algorithm often behaves better than other algorithm in the SIMPLE-family. As far as the boundary condition of the pressure equation is concerned [26], Blosch et al. [27] demonstrated that the implementation of the mass conservation condition in the SIMPLE-family algorithm implied the Neumann condition for the pressure correction equation. Convergence criterion for the velocities is that the maximum mass residual of the cells divided by the maximum residual of the first 5 iterations is less than 10^{-7}. Our numerical practice shows that once the above condition is satisfied, the scaled residuals of momentum and energy equations are all less than 10^{-8}.

The spanwise averaged Nusselt number and frictional factor may be calculated by:

$$Nu_x = \frac{\Phi_x}{[T_w - T_{mb}(x)] \cdot l \cdot dx} \cdot \frac{D_e}{\lambda} \tag{4}$$

In which

$$\Phi_x = \int\int \rho c_p u(x,y,z) \cdot T(x,y,z)\, dy\, dz|_{x+dx} - \int\int \rho c_p u(x,y,z) \cdot T(x,y,z)\, dy\, dz|_x \tag{5}$$

$$T_{mb}(x) = \frac{1}{2}[T_b(x + dx) + T_b(x)] \tag{6}$$

$$T_b(x) = \frac{\int\int T(x,y,z) \cdot u(x,y,z)\, dy\, dz}{\int\int u(x,y,z)\, dy\, dz} \tag{7}$$

$$f = \frac{dp_x}{\frac{1}{2}\rho u_0^2} \frac{D_e}{dx} \tag{8}$$

In order to obtain an appropriate grid system, a grid refinement was conducted to investigate the influence of grid density on the computational results. Three grid systems were tested. The nodes $G_y \times G_z$ of the cross-section are 20×40, 40×80 and 40×100, respectively, and the width of the cells in x-direction are 2–4 times of that in y-direction. It is found that the Nusselt number in the developed region ($x_{in}/D_e > 20$) of the duct at the grid system 40×80, and the cells width in x-direction is 4 times of that in y-direction yields 2% lower than that at the finest grid system 40×100, and the cells width in x-direction is 2 times of that in y-direction. Thus the grid system 40×80, and the cells width in x-direction is 4 times of that in y-direction was adopted to save the computer resources. The Numerical method validation was conducted on this grid system.

Table 1
Comparison of the computational results for Nusselt number in developed region with theoretical solutions

	Theoretical solutions [21]	Present study	Relative error (%)
Nu_x	4.44	4.476	0.8
fRe	73	71.6	1.9

Fig. 1b shows the variation of spanwise averaged Nusselt number along the length of the channel under the conditions that the downstream extended region of the computational domain are $5D_e$ and $10D_e$, respectively. It shows little difference in Nu_x between the two cases. From the figure it is concluded that the fully developed results have been obtained. The fully developed Nusselt number is 4.476. The comparison of the spanwise average Nusselt number and the duct frictional factor at different Reynolds number in the fully developed section of the duct between the theoretical solutions and computational results are listed in Table 1. The relative errors of Nu_x and $f \cdot Re$ are less than 0.8% and 1.9%, respectively. The preliminary computation shows the feasibility of the adopted numerical techniques and they will be used in the following simulations of the flow and heat transfer in the channel with LVG.

4. Effects of the thickness of LVG and the punched holes on the flow and heat transfer of laminar channel

4.1. Physical model and mathematical descriptions of the rectangular channel with LVG

The studied channel is supposed to be formed by two neighboring fins in the heat exchanger. The LVG with given shape and size is a special heat transfer surface which is punched out from the fin surface as show in Fig. 2. As an example, here a pair of rectangular winglets are taken as the longitudinal vortex generator (RWLVG) in the fin channel. Considering the symmetry of the channel, only one half of the channel is numerically computed as shown in Fig. 2a. Note that there are punched holes both in the bottom and top fin surfaces. In this situation, the thickness of LVG should be the same of the fin. The cross-section of $B \times H$ is 160×40 mm. The length of the channel is 400 mm. The ratio of the fin pitch to the fin thickness in the present study is approximately 10. Thus, the thickness of the LVG is determined to be 4 mm. The height of the rectangular LVG is 20 mm that is one half of the channel height, and its length is 40 mm and the attack angle denoted as β is 30°. The location of RWLVG is determined by the coordinates of s (=80 mm) and a (=10 mm) as shown in Fig. 2b. Thus the RWLVG is located in the developing flow region. The outlet downstream region is extended 600 mm that is 15 times of the channel height, so that the fully developed boundary condition is employed at the computational domain outlet.

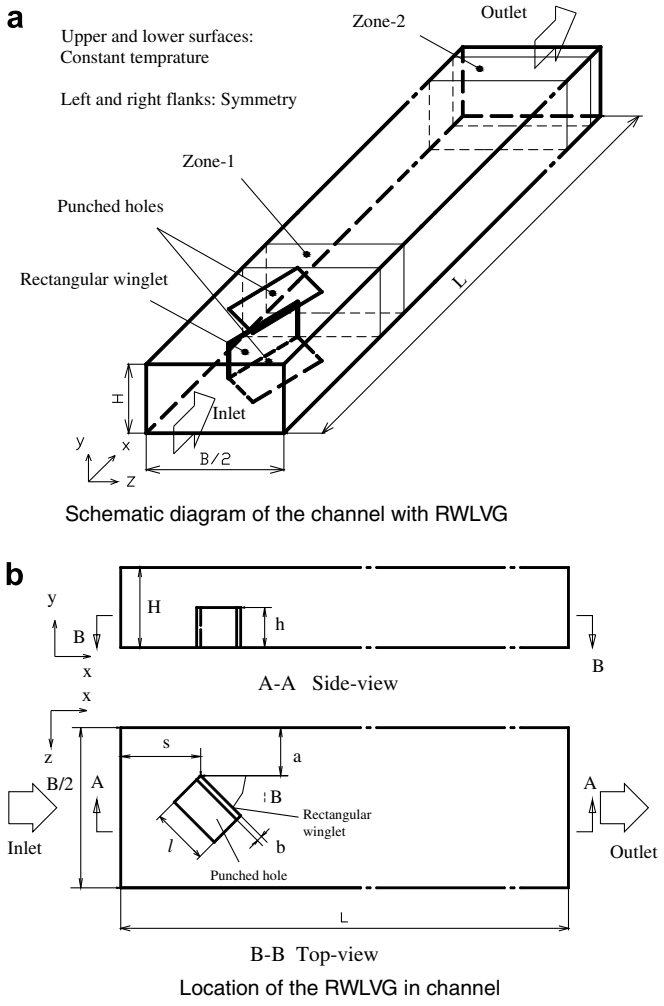

Fig. 2. Schematic diagram of the channel with LVG.

The governing equations can still be described by Eqs. (1)–(3). The boundary conditions are summarized as follows:

Uniform axial velocity and temperature profiles are assigned for the inlet. Non-slip boundary condition and fixed temperature are imposed for the fin surfaces of $y = 0$ and $y = H$. The surfaces of $z = 0$ and $z = B/2$ are symmetrical plane. Symmetrical boundary condition is also assigned to the lateral surfaces of the extended region downstream. Fully developed boundary is imposed for the outlet.

The periodic boundary conditions will be employed for the holes on the fin surfaces. The uniform temperature wall condition is used for fin surfaces when the holes are not considered.

For the wall of the rectangular winglet, non-slip boundary condition is used, and its temperature is assumed to be the same with that of the fin wall.

The computational fluid is also the incompressible air with Prandtl number of 0.71. Reynolds number based on the inlet uniform velocity and 2 times of the channel height, 2H is 1600.

It should be noted here that for the comparison purpose computation is also conducted for the LVG without thickness. Actually this is simulated by a very thin thickness of 0.1 mm which is far less than the thickness of 4 mm. In such a way the viscous retarding effects of the LVG wall can be correctly simulated while the other effects of the LVG thickness can be neglected. Thus either the governing equations and the boundary conditions or the grid generation technique for the cases with and without LVG thickness are the same, and the only difference is the grid number in the thickness of LVG. In addition also for the comparison purpose simulation is conducted for the case without punched hole, by changing the boundary conditions of velocity at the hole area from periodic to no-slip for velocity.

4.2. Computational results and discussion

The existence of the attack angle between the RWLVG and the main flow makes the computational region complicated. In order to accurately simulate the shape of the RWLVG, the block-structured technique [28] is used to generate the grids in the numerical simulation. Fig. 3 shows the profile of the meshes near to the RWLVG. The region near to the RWLVG is divided into 12 sub-regions. The node number of each side is adjustable to control mesh density so that the mesh of the region near the RWLVG and fin wall is denser. An effort was undertaken to find the suitable grid density (about 300,000 cells in total) and to obtain the grid-independent results.

4.2.1. Effects of the punched holes on the flow and heat transfer

As indicated above, the cases with or without punched holes in given thickness of the RWLVG are numerically simulated. Fig. 4 shows the variations of spanwise averaged Nu_x along the streamwise location x/H for the two cases. From Fig. 4, we can find that the punched holes mainly influence the profile of Nu_x near the holes. It is very inter-

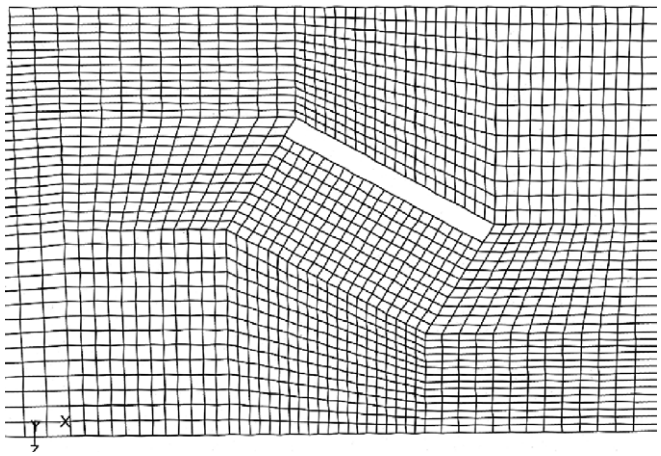

Fig. 3. The profile of meshes near the RWLVG.

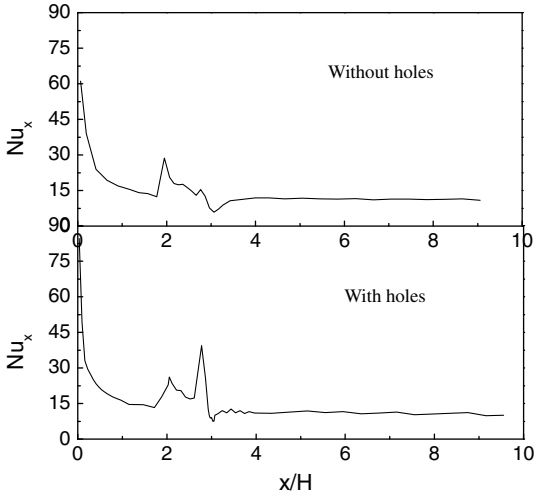

Fig. 4. The influence of punched holes on spanwise averaged Nusselt number.

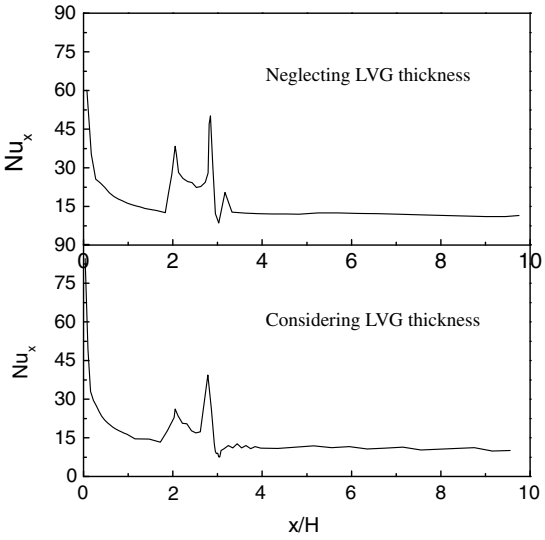

Fig. 5. The influence of RWLVG thickness on spanwise averaged Nusselt number.

esting to point that for the both cases Nu_x almost does not vary along x/H in the downstream of the RWLVG. This trend is not found in the channel without LVG in which Nu_x decreases along x/H until the flow is fully developed. This may be explained by that fact that the LV generated by the RWLVG swirls and disturbs the flow and enhances the heat transfer in the downstream. The average Nusselt number of the whole channel with holes is slightly higher than (by about 1.1%) that without holes. The numerical results also indicate the average fictional factor of the whole channel with holes is slightly lower than that without holes, which is about 1.2%. Flow visualization in channels with a pair of delta winglet punched out from an aluminum plate was conducted in our study, the details of which will be shown in the companion paper [20]. It was observed that air flow in the upper channel turned into the lower channel through the punched holes, bringing about disturbance to the air flow in the lower channel. This may be the reason of the slight heat transfer enhancement. At the same time, the form drag of the delta winglet pair may be reduced due to the by-pass air flow through the holes.

4.2.2. Effect of LVG thickness on the flow and heat transfer

The effect of LVG thickness on the heat transfer in the channel with punched holes is shown in Fig. 5 where the Nu_x profiles in the conditions of considering or neglecting the thickness of RWLVG are presented. It shows that the thickness of LVG mainly influences the heat transfer near the LVG. The average Nusselt number of the whole channel in the condition of considering the thickness of LVG is lower than that of neglecting the thickness of LVG by about 4.1%. The numerical results indicate that the thickness of LVG has little influence on the average fictional factor of the channel at the present condition. The reason of almost the same pressure drop is that the total pressure drop of the channel is mainly caused by the form drag of LVG in which the attack angle and frontal area of LVG are the decisive factors, not the thickness of LVG. The reduction in heat transfer of the much thicker LVG may be attributed to the fact that the existence of the solid region of LVG thickness produces some negative effect on the generated LVG either in its size or in its intensity.

The present results tell us that the punched holes and the LVG thickness mainly influence the flow and the heat transfer near the LVG. These physical factors should be taken into account in the following simulations of the influence of the longitudinal vortex on the flow and heat transfer characteristics.

5. Mechanism of the heat transfer augmentation by LV

The LV is generated because the velocity boundary layer separates from the side-edge of RWLVG when fluid flows over it. From the traditional viewpoints, the mechanism of the heat transfer enhancement by the LVs is explained as that the generated longitudinal vortices disturb, swirl and mix the fluid flow, break the boundary layer developing and make it thinner. As a matter of fact, the secondary flow generated by the LVs changes the flow and temperature field, that is to say, the inherent flow and heat transfer connection is changed. It is the authors consideration that the essence of the heat transfer enhancement by the LV should be explained from the field synergy principle developed quite recently. For the readers convenience a brief introduction of FSP is given below.

5.1. A brief review of the field synergy principle

A novel concept called field synergy principle for the boundary-layer flow was firstly proposed by Guo and his co-workers [29]. Starting from the energy equation, the authors integrated the equation through the thickness of the boundary and obtained a results in which it is shown

that the heat transfer rate depends on the inner production of local velocity vector and temperature gradient. Later Guo et al. [30] obtained a non-dimensional correlation of local Nusselt number from a two-dimensional boundary layer flow. The non-dimensional correlation is written as:

$$Nu_x = Re_x Pr \int_0^1 (U \cdot \mathrm{grad}\,\Theta)\,\mathrm{d}Y \tag{9}$$

where Nu_x is local Nusselt number, Re_x is local Reynolds number, Pr is fluid Prandtl number, U is the non-dimensional velocity vector, Y is the non-dimensional distance normal to the wall and gradΘ is the non-dimensional temperature gradient.

From the vector theory the dot product term of vectors may be written as:

$$U \cdot \mathrm{grad}\,\Theta = |U||\mathrm{grad}\,\Theta|\cos\theta \tag{10}$$

in which θ is the intersection angle between the local velocity vector and temperature gradient, called as synergy angle.

From Eqs. (9) and (10), it can be clearly observed that for the same oncoming flow velocity and total temperature difference between the wall and the oncoming flow the smaller the intersection of the local velocity vector and the temperature gradient, the larger the heat transfer rate. This is the basic idea of field synergy principle. Thus for the convection heat transfer, at least for the single phase case, reducing the intersection angle between the velocity vector and temperature gradient is the basic mechanism for enhancing convective heat transfer. This concept was extended from parabolic flow to elliptic flow by Tao et al. [31] and numerical verifications were provided in [32] showing that the existing three mechanisms of convective heat transfer enhancement actually lead to the reduction of the intersection angle between the local velocity vector and temperature gradient. A comprehensive review of recent studies of the field synergy principle was provided by Guo et al. [33].

The major purpose of the present study is to apply the field synergy principle to explain the essence of heat transfer enhancement by LVs, answer the question such as why LVs can lead to the integral heat transfer enhancement while TVs just lead to the local heat transfer enhancement.

From Eq. (10) we can see that synergy angle is a function of velocity vector and temperature gradient, so it is related to the local position. The local synergy angle can be calculated by Eq. (11). The volume average synergy angle in the whole flow field can be determined by Eq. (12).

$$\theta = \arccos\left(\frac{U \cdot \mathrm{grad}\,\Theta}{|U||\mathrm{grad}\,\Theta|}\right), \tag{11}$$

$$\theta_\mathrm{m} = \frac{\int\int\int_V \theta\,\mathrm{d}v}{\int\int\int_V \mathrm{d}v} \tag{12}$$

There are a lot of factors which influence the heat transfer enhancement by the LV such as Reynolds number, the attack angle of the RWLVG, the shape and geometric sizes of the RWLVG, the location of the RWLVG in the channel, etc. We will study the effects of these factors on the average Nusselt number, average synergy angle, average friction factors by numerical method to verify the field synergy principle and further reveal the inherent mechanism of heat transfer enhancement by the LVs. The average Nusselt number and friction factor are calculated by the following equations:

$$Nu_\mathrm{m} = \frac{\Phi}{A \cdot (T_\mathrm{w} - T_\mathrm{f})} \cdot \frac{2H}{\lambda} \tag{13}$$

where Φ is the total heat transfer rate between the air and solid wall(including fin and LVG surfaces), T_f is the arithmetic average bulk temperature (defined in Eq. (7)) of the channel inlet and outlet, and A is the total heat transfer area.

$$f = \frac{\Delta p}{\frac{1}{2}\rho u_0^2}\frac{2H}{L} \tag{14}$$

where Δp is the total pressure drop between the inlet and outlet.

5.2. Effects of LVs on the velocity and temperature field of the channel

The cross-section of the computed channel is $B \times H = 0.08 \times 0.02$ m, and the channel length is 0.3 m. First, the flow and heat transfer in the channel without RWLVG is numerically computed under four different Reynolds numbers: 800, 1600, 2400 and 3000, respectively. These results are used as the database to check the effectiveness of RWLVG in the heat transfer enhancement. According to Fiebig [2], the generated vortices are mainly longitudinal ones when the attack angle of the VG is smaller than 45°, while the transverse component in the generated vortices increases gradually with increasing the attack angle when the attack angle of VG is larger than 45°. When the attack angle reaches 90°, the generated vortices will be transverse ones only. Under the conditions of the given sizes and location of the RWLVG ($l = 0.02$ m, $h = 0.01$ m, $b = 0.002$ m, $s = 0.08$ m, $a = 0.01$ m as shown in Fig. 3), the convection heat transfer in the channel with RWLVG at the different attack angles of 15°, 30°, 45°, 60° and 90°, under four different Reynolds numbers of 800, 1600, 2400 and 3000, respectively, are computed.

As stated before the secondary flow generated by the LVs changes the flow and temperature field, that is to say, the inherent flow and heat transfer connection is changed. The flow and temperature fields of the case at the condition of $Re = 1600$ and $\beta = 30°$ are presented in Fig. 6 where the axial velocity contour at the different cross-sections of channel are presented. Fig. 7 shows the secondary flow at the different cross-sections in the downstream of RWLVG. From Figs. 6 and 7 we can see the evolving process of the longitudinal vortices. The first cross-section of $x = 0.04$ m in Fig. 6 is located in the front of RWLVG and the axial velocity is layered. The second cross-section

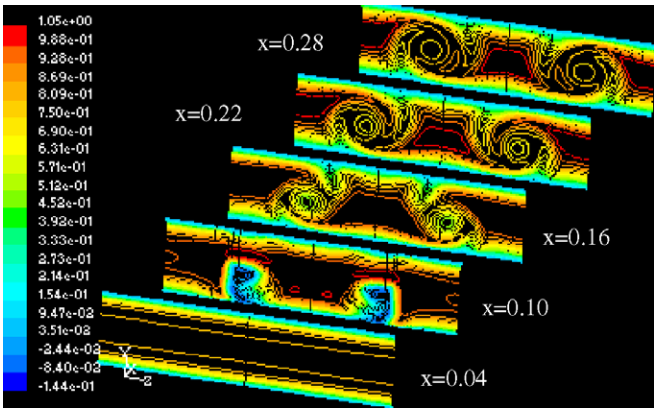

Fig. 6. Axial velocity profiles at the different cross-section ($Re = 1600$, $\beta = 30^\circ$, x in m).

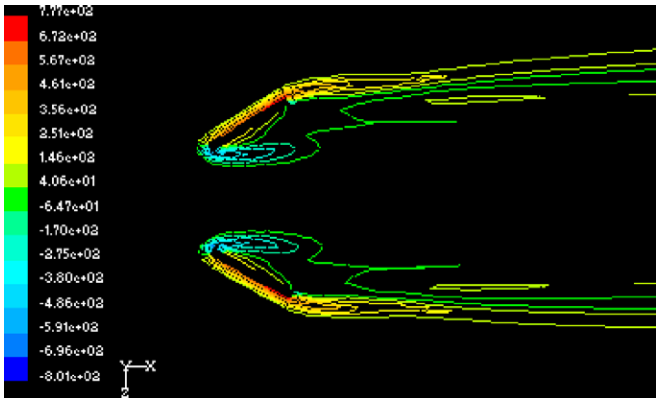

Fig. 8. Contour of y-vorticity around the RWLVG at the section of $y = 0.2$ H.

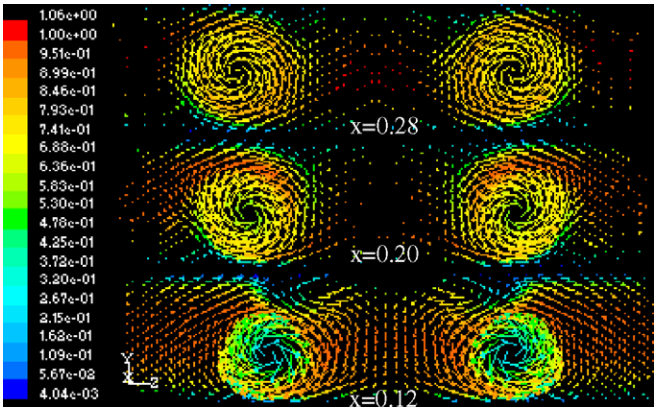

Fig. 7. Longitudinal vortices at the different cross-sections (x in m).

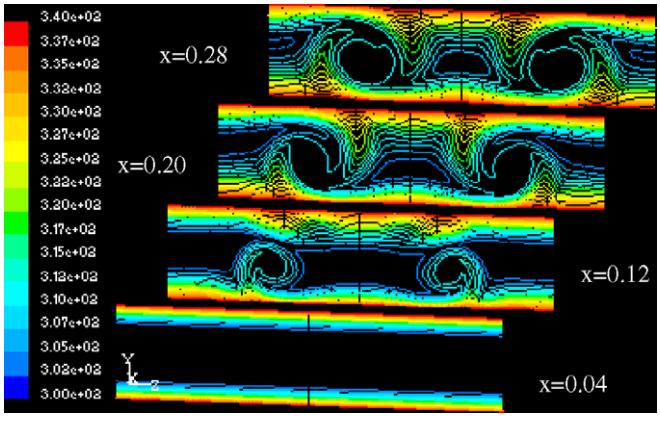

Fig. 9. Temperature profiles at the different cross-sections (x in m).

of $x = 0.1$ m just lies at the position of RWLVG, where reverse flow occurs (the axial velocity is negative). From Fig. 7 we can see a pair of longitudinal vortices with stronger strength is generated at the cross-section of $x = 0.12$ m, which is next to the trailing edge of RWLVG. Although the velocity magnitude in the center of the LVs is relatively lower(see Fig. 6), the secondary flow is very strong(see Fig. 7). Comparing the velocity distributions on the different cross-sections we can see that the influencing range of the LVs in transverse direction is getting wider and insisting on in the longitudinal direction. The secondary flow velocity is decreasing gradually due to the diffusion caused by the viscosity of fluid. For the cases studied the maximum transverse velocity of the longitudinal vortex reaches about 0.3367 m/s and 0.3773 m/s in y- and z-directions, respectively. Both of them are about one half of the uniform inlet velocity (0.7089 m/s). Fig. 8 shows the contours of y-vorticity (vortex lines) on the plane of $y = 0.2$ H. From this figure we can observed that the transverse vortices are also generated at the leading and trailing edges of the RWLVG when fluid flows over the RWLVG. This may explains why reverse flow occurs in the cross-section of $x = 0.1$ m in Fig. 6. Transverse vortex can enhance local heat transfer, so this is one of the reasons why Nu_x always has a peak at the leading and trailing edges of the RWLVG in Figs. 4 and 5.

Fig. 9 shows the temperature profiles at the different cross-sections in which the locations of the last three sections are the same with those in Fig. 7. It clearly shows that the longitudinal vortices lead to the deformation of the temperature profiles in the flow channel. In the first cross-section ($x = 0.04$ m) which is located at the front of RWLVG, the temperature profile is layered because of the laminar flow characteristics. In the second section ($x = 0.12$ m) which is next to the trailing edges of RWLVGs, the temperature field has been influenced by the LVs. The variations of temperature profile from the second section to the fourth section tell us that the LVs are spreading gradually and leading to the mixing of fluid in the channel. Comparing Fig. 9 with Fig. 7, we can see that, the temperature boundary layer becomes thinner in the areas where the secondary flow washes upon the wall. While the temperature boundary layer becomes thicker in the areas where the secondary flow is away from the wall.

Fig. 10 shows the variation of average pressure in x-direction. We can see from this figure that a steep pressure drop occurs at the inlet of channel, and a much steeper pressure drop occurs around the RWLVGs because of its

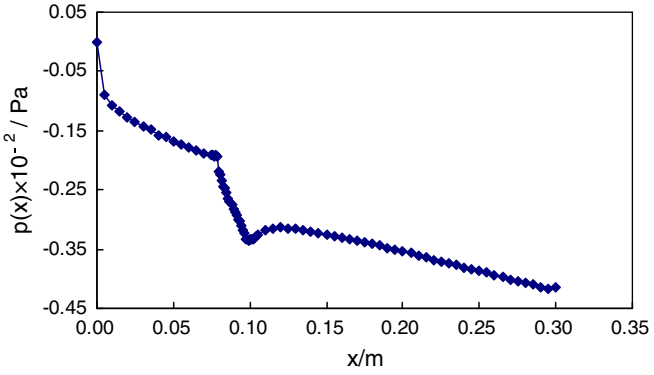

Fig. 10. Variation of average pressure in the main flow direction ($Re = 1600$, $\beta = 30°$).

form drag. Upon leaving the RWLVG part because of the increase in the cross-section flow area the fluid pressure rises again, then it decreases and gradually exhibits a more or less linear variation character.

At this point a question may arise as how about the comparison of our numerical prediction with the flow visualization results in the open literatures. In fact such a comparison is quite difficult because the experimental conditions of flow visualization were often not clearly stated in the open literature. Furthermore, most experimental work was conducted for turbulent flow, while the present work is limited to the laminar one. Being aware of such situation, the present authors conducted some visualization and experimental measurement the details of which will be presented in [20]. Because of some failure in our experimental techniques we could not clearly recorded the flow pattern of the generated longitudinal vortex, however, we have successfully obtained the over heat transfer results which will be presented in the companion paper. In addition, we have compared our numerical predicted vortex evolution along the flow direction with [34] by Kahallaki, Russeil and Baudoin. In their computation, the LVG attack angle was 18° and the computation was conducted for turbulent flow in a rectangular duct with a pair of LVG. As far as the axial evolution process of the pair of vortices is concerned the two predictions agree qualitatively quite well.

5.3. Effects of reynolds number and attack angle of RWLVG on channel flow and heat transfer

Fig. 11 shows the relationships of the heat transfer enhancement (Nu_m/Nu_0) vs. Reynolds numbers for the channels with RWLVG at different attack angles. From the figures following features may be noted. First, as it can be expected, the Nusselt number increases with increasing Reynolds number. Second, as far as the heat transfer enhancement is concerned it can be clearly observed that Nu_m/Nu_0 for the case with attack angle of 45° is always larger than those for the cases with other attack angles in the whole range of Reynolds number. This means that RWLVG with attack angle of 45° provides the better effectiveness of the heat transfer enhancement, the next is the cases with attack angle of 60°, and then 30°, 90° and 15° in order. This result indicates that the VG does have effect to enhance heat transfer. However, due to the different attack angles, the strength of the vortex, vortex components (LV or TV) and its influence range are different. In fact vortices generated by VGs have changed the velocity and temperature distributions in channels. So the synergy angles in the channels with RWLVG at different attack angles have been changed too. Third, the relationships of the average synergy angles vs. Reynolds numbers of the different six cases (plain channel and 5 channels with RWLVG at different attack angles) shown in Fig. 11. It shows that the synergy angle for the case with attack angle of 45° is always lower than those for the cases with other attack angles in the whole range of Reynolds number.

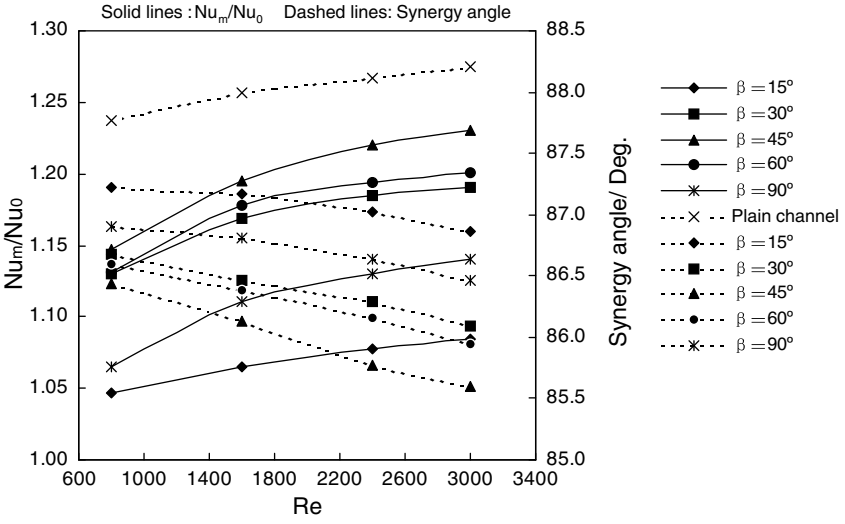

Fig. 11. Nu_m/Nu_0 and synergy angle vs. Reynolds number for the six cases.

Table 2
Comparisons of the field synergy in different zones of the channels

Zone	Average synergy angle θ_m (°)					
	Plain channel	$\beta = 15°$	$\beta = 30°$	$\beta = 45°$	$\beta = 60°$	$\beta = 90°$
Zone-1	88.525	87.515	86.654	85.679	85.137	85.081
Zone-2	89.264	88.743	88.402	88.259	88.552	88.861

The next is the case with RWLVG at the attack angle of 60° and then 30°, 90° and 15° in order. The plain channel without LVG has the largest synergy angle among the six cases. The finding that at the same Reynolds number the smaller the average synergy angle the larger the Nusselt number is completely consistent with the field synergy principle. In other words, when the second flow generated by vortex generators results in the reduction of the intersection angle between the velocity and fluid temperature gradient, the heat transfer in the present channels will be enhanced. Fourth, it is interesting to note that the synergy angle of the plain channel without LVG increases with increasing Reynolds number, while decreases for the channel with LVG. Thus we can conclude that the increase of Nusselt number with increasing Reynolds number for the channel with suitable LVG not only owes to the increase of velocity, but also owes to the improvement of synergy between the velocity and temperature field.

To compare the synergy improvement by the LV and TV, two zones named zone-1 and zone-2 in the channel are selected as shown in Fig. 2. Zone-1 is located near VG, and its range is $x = 0.08$–0.11 m. Zone-2 is located near the outlet of the channel, and its range is $x = 0.25$–0.28 m. The average synergy angles in the two zones are calculated for the plain channel and the other channels with the VGs at different attack angles. The results are provided in Table 2. It shows that the synergy angle of zone-1 for the channel with rectangular winglet pair at attack angle of 90° is the lowest among the six cases, the next is the cases of 60°, and then 45°, 30° and15° in order. The synergy angle of zone-1 for plain channel is the largest. However, in the zone-2, the synergy angle for the channel with rectangular winglet pair at attack angle of 45° is the lowest among the six cases, the next is the cases of 30°, and then 60°, 15° and 90°. Of course the synergy angle of zone-2 for plain channel is the largest yet. These findings tell us that the LVs (the ones generated by rectangular winglet pair at attack angle of 45° or 30° in the above cases) improve the synergy between velocity and temperature field not only in the region near the LVG but also in the large downstream region of LVG. So LVs enable to enhance the global heat transfer of channel. However, the TV (the one generated by rectangular winglet pair at attack angle of 90° in the above cases) only improves the synergy in the region near the VG. So the TV can only enhance the local heat transfer of channel.

It is interested to note here that even though the heat transfer enhancement of the LVG at attack angle 45° is better than that at the other attack angles studied, it still cannot be regarded the best one for the conditions studied. Such best attack angle is highly geometric dependent, and in order to find it a detailed numerical search should be conducted. For the conditions studied the search may be conducted with the range of 30°–60°. Since the major concern of the present study is to reveal the essence of heat transfer enhancement by the LVG, and single LVG is rarely used in practice, such numerical search was not performed.

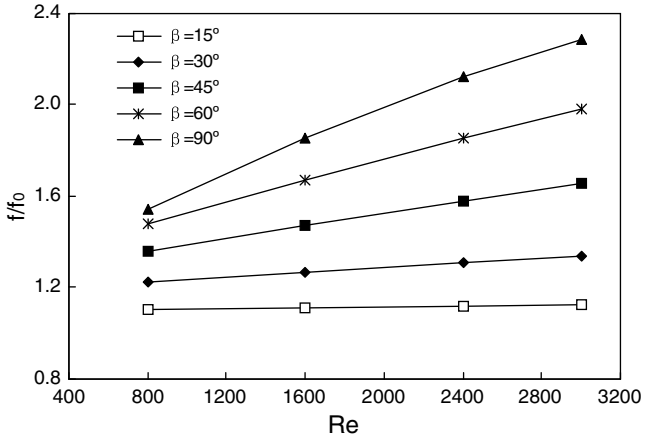

Fig. 12. f/f_0 vs. Reynolds number for the six cases.

RWLVG enhances the heat transfer of the channel as well as results in an extra pressure drop due to its form drag. Fig. 12 shows the increases of friction factor in the channel with RWLVG at different attack angle vs. Reynolds number. With the increase of β, friction factor increases rapidly. This is because with the increase of β, the frontal area of LVG increases, thus the form drag of LVG increases significantly.

6. Conclusions

Numerical study on laminar convection heat transfer in the channel with punched rectangular winglet pair is carried out. The mechanism of the heat transfer augmentation by the LVs is discussed based on the field synergy principle. The following conclusions are obtained.

(1) The punched hole under the LVG mainly influences the heat transfer of the region near the LVG. The average Nusselt number of the whole channel with

holes is slightly higher than that without holes. The average friction factor of the whole channel with holes is slightly lower than that without holes.

(2) The thickness of LVG mainly influences the flow and heat transfer near the LVG too. The average Nusselt number of the whole channel at the condition of considering the thickness of LVG is lower than that of the case neglecting the thickness of LVG. The thickness of LVG has little influence on the average friction factor of the channel at the present condition.

(3) The vortex generator with the attack angle of 45° always provides the better effectiveness of heat transfer enhancement, the next is that with attack angle of 60°, and then 30°, 90° and 15° in order.

(4) The pressure drop of the channel with the LVG increases rapidly with the increase of the attack angle of the LVG.

(5) The essence of heat transfer enhancement by the vortex generator is due to the improvement in the field synergy between the velocity and the temperature gradient. That is, when the second flow generated by the vortex generators results in the reduction of the intersection angle between the velocity and fluid temperature gradient, the heat transfer in the present channels will be enhanced.

(6) Synergy angle increases with increasing Reynolds number for the plain channel without the LVG, while decreases for the channel with the LVG.

(7) The LVs improve the synergy between velocity and temperature gradient not only in the region near LVG but also in the large downstream region of the LVG. So the LVs enable to enhance the global heat transfer of channel. The TVs only improve the synergy in the region near the VG. So the TVs can only enhance the channel local heat transfer.

Acknowledgements

Supports from the National Basic Research of China (973 Program) (2007CB 206902), and the National Natural Science Foundation of China (No. 50476046) are greatly appreciated.

References

[1] C.C. Wang, Technical review – a survey of recent patents of fin-and-tube heat exchangers, J. Enhanced Heat Transfer 7 (5) (2000) 333–345.

[2] M. Fiebig, Vortices and heat transfer, Zeit. Angew. Math. Mech. 77 (1) (1997) 3–18.

[3] G.B. Schubauuer, W.G. Spangenberg, Forced mixing in boundary layers, J. Fluid Mech. 8 (1960) 10–31.

[4] T.R. Johnson, P.N. Joubert, The Influence of vortex generators on drag and heat transfer from a circular cylinder normal to an airstream, J. Heat Transfer 91 (1969) 91–99.

[5] A.Y. Turk, G.H. Junkhan, Heat Transfer enhancement downstream of vortex generators on a flat plate, in: Proceedings of the Eighth International Heat Transfer Conference, vol. 6, 1986, pp. 2903–2908.

[6] P.A. Eibeck, J.K. Eaton, Heat transfer effects of a longitudinal vortex embedded in a turbulent boundary layer, J. Heat Transfer 109 (1987) 16–24.

[7] W.R. Pauley, J.K. Eaton, Experimental study of the development of longitudinal vortex pairs embedded in a turbulent boundary layer, AIAAJ 26 (1988) 816–823.

[8] T. Shizawa, J.K. Eaton, Turbulence measurements for a longitudinal vortex interacting with a three-dimensional turbulent boundary layer, AIAAJ 30 (1992) 49–55.

[9] A.M. Jacobi, R.K. Shah, Heat transfer surface enhancement through the use of longitudinal vortices: a review of recent progress, Exp. Thermal Fluid Sci. 11 (1995) 295–309.

[10] M. Fiebig, P. Kallweit, N.K. Mitra, Wing type vortex generators for heat transfer enhancement, in: Proceedings of the Eighth International Heat Transfer Conference, vol. 6, 1986, pp. 2909–2913.

[11] M. Fiebig, P. Kallweit, N.K. Mitra, S. Tiggelbeck, Heat transfer enhancement and drag by longitudinal vortex generators in channel flow, Exp. Thermal Fluid Sci. 4 (1991) 103–114.

[12] S. Tiggelbeck, N.K. Mitra, M. Fiebig, Experimental investigations of heat transfer enhancement and flow losses in a channel with double rows of longitudinal vortex generators, J. Heat Mass Transfer 36 (1993) 2327–2337.

[13] G. Biswas, N.K. Mitra, M. Fiebig, Computation of laminar mixed convection flow in a channel with wing type built-in obstacles, J. Thermophys. 3 (1989) 447–453.

[14] G. Biswas, H. Chattopadhyay, Heat transfer in a channel with built-in wing type vortex generators, Int. J. Heat Mass Transfer 35 (1992) 803–914.

[15] G. Biswas, K. Torii, D. Fuji, K. Nishino, Numerical and experimental determination of flow structure and heat transfer effects of longitudinal vortices in a channel flow, Int. J. Heat Mass Transfer 39 (1996) 3441–3451.

[16] M. Fiebig, U. Brockmeier, N.K. Mitra, T. Guntermann, Structure of velocity and temperature fields in laminar channel flows with vortex generators, Num. Heat Transfer, Part A 15 (1989) 281–302.

[17] A.K. Saha, K. Muralidhar, G. Biswas, Vortex structures and kinetic energy budget in two-dimensional flow past a square cylinder, Comput. Fluids 29 (2000) 669–694.

[18] A. Sohankar, L. Davidson, Effect of inclined vortex generators on heat transfer enhancement in a three-dimensional channel, Num. Heat Transfer, part A 39 (2001) 443–448.

[19] J.D. Chung, B.K. Park, J.S. Lee, The combined effects of angle of attack and louver angle of a winglet pair on heat transfer enhancement, J. Enhanced Heat Transfer 10 (1) (2003) 31–43.

[20] J.M. Wu, W.Q. Tao, Numerical study on laminar convection heat transfer in a rectangular channel with longitudinal vortex generator, Part B: Parametric study of major influence factors, Int. J. Heat Mass Transfer, in press.

[21] Y.P. Cheng, Z.G. Qu, W.Q. Tao, Y.L. He, Numerical design of efficient slotted fin surface based on the field synergy principle, Numer. Heat Transfer, Part A 45 (2004) 517–538.

[22] F.P. Incropera, D.P. Dewitt, Fundamental of Heat and Mass Transfer, fifth ed., Wiley, New York, 2002.

[23] J.P. van Doormaal, G.D. Raithby, Enhancement of the SIMPLE method for predicting incompressible fluid flow, Numer. Heat Transfer 7 (1984) 147–163.

[24] D.S. Jang, R. Jelti, S. Archaya, Comparison of the PISO, SIMPLER and SIMPLEC algorithms for the treatment of pressure-velovity coupling in steady flow problems, Numer. Heat Transfer 11 (1986) 209–228.

[25] F. Moukalled, M. Darwish, A unified formulation of the segregated class of algorithm for fluid flow at all speeds, Numer. Heat Transfer, Part B 44 (2000) 103–139.

[26] P.M. Gresho, A simple question to SIMPLE users, Numer. Heat Transfer, Part A 20 (1990) 123.

[27] E. Blosch, W. Shyy, R. Smith, The role of mass conservation in pressure-based algorithm, Numer. Heat Transfer, Part B 24 (1993) 415–429.

[28] W.Q. Tao, Recent Advances in Computational Heat Transfer, Science Press, Beijing, 2000, pp. 43–63.
[29] Z.Y. Guo, D.Y. Li, B.X. Wang, A novel concept for convective heat transfer enhancement, Int. J. Heat Mass Transfer 41 (1998) 2221–2225.
[30] Z.Y. Guo, S. Wang, Novel concept and approaches of heat transfer enhancement, in: Proceedings of Symposium on Energy and Engineering, Begell House, New York, 2000, pp. 118–126.
[31] W.Q. Tao, Z.Y. Guo, B.X. Wang, Field synergy principle for enhancing convective heat transfer – its extension and numerical verifications, Int. J. Heat Mass Transfer 45 (2002) 3849–3856.
[32] W.Q. Tao, Y.L. He, Q.W. Wang, Z.G. Qu, F.Q. Song, A unified analysis on enhancing convective heat transfer with field synergy principle, Int. J. Heat Mass Transfer 45 (2002) 4871–4879.
[33] Z.Y. Guo, W.Q. Tao, R.K. Shah, The field synergy (coordination) principle and its applications in enhancing single phase convective heat transfer, Int. J. Heat Mass Transfer (2005) 1797–1807.
[34] K. Khallaki, R. Russeil, B. Baudoin, Simulation of formation mechanism and transport of longitudinal vortices in 3-D boundary layer, in: Proceedings of Fifth International Conference on Enhanced, Compact and Ultra-Compact Heat Exchangers: Science, Engineering and technology, Engineering Conference International, Hoboken, NJ, USA. CHE 2005-58, 2005, pp. 442–447.